

# Molecular dynamics and information on possible sites of interaction of intramyocellular metabolites in vivo from resolved dipolar couplings in localized $^1\text{H}$ NMR spectra

Leif Schröder<sup>a,\*</sup>, Christian Schmitz<sup>b</sup>, Peter Bachert<sup>a,\*</sup>

<sup>a</sup> *Abteilung Medizinische Physik in der Radiologie, Deutsches Krebsforschungszentrum (dkfz), D-69120 Heidelberg, Germany*

<sup>b</sup> *Biophysikalische Chemie, Institut für Physikalische Chemie, Universität Heidelberg, D-69120 Heidelberg, Germany*

Received 23 June 2004; revised 18 August 2004

Available online 25 September 2004

## Abstract

Proton NMR resonances of the endogenous metabolites creatine and phosphocreatine ((P)Cr), taurine (Tau), and carnosine (Cs,  $\beta$ -alanyl-L-histidine) were studied with regard to residual dipolar couplings and molecular mobility. We present an analysis of the direct  $^1\text{H}$ – $^1\text{H}$  interaction that provides information on motional reorientation of subgroups in these molecules in vivo. For this purpose, localized  $^1\text{H}$  NMR experiments were performed on m. gastrocnemius of healthy volunteers using a 1.5-T clinical whole-body MR scanner. We evaluated the observable dipolar coupling strength  $SD_0$  ( $S$  = order parameter) of the (P)Cr-methyl triplet and the Tau-methylene doublet by means of the apparent line splitting. These were compared to the dipolar coupling strength of the (P)Cr-methylene doublet. In contrast to the aliphatic protons of (P)Cr and Tau, the aromatic H2 ( $\delta = 8$  ppm) and H4 ( $\delta = 7$  ppm) protons of the imidazole ring of Cs exhibit second-order spectra at 1.5 T. This effect is the consequence of incomplete transition from Zeeman to Paschen-Back regime and allows a determination of  $SD_0$  from H2 and H4 of Cs as an alternative to evaluating the multiplet splitting which can be measured directly in high-resolution  $^1\text{H}$  NMR spectra. Experimental data showed striking differences in the mobility of the metabolites when the dipolar coupling constant  $D_0$  (calculated with the internuclear distance known from molecular geometry in the case of complete absence of molecular dynamics and motion) is used for comparison. The aliphatic signals involve very small order parameters  $S \approx (1.4 - 3) \times 10^{-4}$  indicating rapid reorientation of the corresponding subgroups in these metabolites. In contrast, analysis of the Cs resonances yielded  $S \approx (113 - 137) \times 10^{-4}$ . Thus, the immobilization of the Cs imidazole ring owing to an anisotropic cellular substructure in human m. gastrocnemius is much more effective than for (P)Cr and Tau subgroups. Furthermore,  $^1\text{H}$  NMR experiments on aqueous model solutions of histidine and *N*-acetyl-L-aspartate (NAA) enabled the assignment of an additional signal component at  $\delta = 8$  ppm of Cs in vivo to the amide group at the peptide bond. The visibility of this proton could result from hydrogen bonding which would agree with the anticipated stronger motional restriction of Cs. Referring to the observation that all dipolar-coupled multiplets resolved in localized in vivo  $^1\text{H}$  NMR spectra of human m. gastrocnemius collapse simultaneously when the fibre structure is tilted towards the magic angle ( $\theta \approx 55^\circ$ ), a common model for molecular confinement in muscle tissue is proposed on the basis of an interaction of the studied metabolites with myocellular membrane phospholipids. © 2004 Elsevier Inc. All rights reserved.

**Keywords:** In vivo  $^1\text{H}$  NMR; Creatine; Taurine; Carnosine; Human calf muscle; Restricted molecular mobility

## 1. Introduction

Direct spin–spin coupling is extremely important for structure analysis in biochemistry by means of NMR spectroscopy (MRS). Ultimately, it provides spatial and dynamical information about molecular groups

\* Corresponding authors. Fax: +49 6221422531 (L. Schröder).

E-mail addresses: [l.schroeder@dkfz-heidelberg.de](mailto:l.schroeder@dkfz-heidelberg.de) (L. Schröder), [p.bachert@dkfz-heidelberg.de](mailto:p.bachert@dkfz-heidelberg.de) (P. Bachert).

URL: [www.dkfz.de/mrspek](http://www.dkfz.de/mrspek) (P. Bachert).

and even macromolecules in liquid phase. Recently, the same interaction came into focus in in vivo applications where  $^1\text{H}$  MRS studies demonstrated that the mobility of small metabolites is partially restricted in human leg muscle tissue and resonances of several compounds were shown to be affected [1–3]. The observation of residual dipolar couplings challenges the common model of an isotropic liquid for the intracellular environment and may also allow the study of the degree of order in living tissue.

One branch of structure analysis employs the dependence on spatial orientation and intermolecular distance of the dipolar interaction to obtain information about the configuration of molecules placed in known nematic phases [4]. In vivo studies of endogenous metabolites can apply this principle vice versa: small molecules like creatine and phosphocreatine ((P)Cr, total creatine) and carnosine (Cs) are probes to explore the degree of alignment if the same molecule is studied in different cellular environments. On the other hand, spectra of different metabolites obtained from the same type of tissue contain information about differences of molecular dynamics. Both approaches are based on the order parameter  $S$  which relates the dipolar coupling constant  $D_0$  expected from the immobile molecule to the experimentally observed constant  $D_{\text{obs}}$ .  $S$  considers time averaging of the orientation of the internuclear vector [1].

The standard method to determine  $D_{\text{obs}}$  is to measure the line splitting  $\Delta\nu$  for different orientations of the anisotropic structure with respect to the static magnetic field  $\vec{B}_0$  [1,5]:

$$\Delta\nu = \frac{3}{2}D_{\text{obs}}(3\cos^2\theta - 1) = \frac{3}{2}SD_0(3\cos^2\theta - 1) =: \frac{3Sk}{2h}, \quad (1)$$

where  $\theta$  is the angle between the time average of the internuclear vector  $\langle\vec{r}_{ik}\rangle$  and the magnetic field  $\vec{B}_0$  (Planck's constant  $h$  is used to transform the coupling strength  $k$  from terms of energy into frequency dimensions). In fact, this relation can only be applied to a specific type of dipolar-coupled nuclear spins, e.g., two isochronous spins, while the quantum mechanics of anisochronous spins yields a different expression [2].

The most prominent case of residual dipolar coupling in vivo so far is the doublet of the methylene resonance of (P)Cr in  $^1\text{H}$  NMR spectra of human calf muscle. Its line splitting was the target of several studies [1,6–8] and the large discrepancy between the expected and observed dipolar coupling constant indicated that the mobility of the  $\text{CH}_2$  group of (P)Cr is not restricted very strongly. Likewise the signals of the two  $\text{CH}_2$  groups of taurine (Tau) which display a common resonance at 1.5 T are also affected by dipolar line splitting [6]. It has been reported recently that there is also a pool of the endogenous dipeptide carnosine ( $\beta$ -alanyl-L-histidine) that is subjected to a residual dipolar interaction [2,9].

The decisive difference between these metabolites is the type of single protons being involved in the intramolecular interaction. While the spectra of (P)Cr and Tau are affected by couplings between magnetically equivalent protons ( $\text{CH}_3$  or  $\text{CH}_2$ ), the imidazole ring protons of Cs undergo a long-range interaction of anisochronous spins that provides information on restricted molecular mobility of the entire ring structure. We emphasize the peculiarity of the Cs spin system: conditions at 1.5 T produce second-order spectra which contain more parameters related to the coupling strength than only the line splitting.

The first aim of the present study is to employ the different parameters of these spectra to determine the order parameters related to the dipolar coupling effects of Cs. The comparison with  $S$  derived for (P)Cr and Tau will demonstrate that the quantum-mechanical treatment of the dynamics of  $\text{CH}_2$ ,  $\text{CH}_3$ , and imidazole ring protons differs in some important details and care has to be taken when indicating the order parameter of these spin systems. To the best of our knowledge, only the line splitting of the (P)Cr doublet was quantified so far in terms of  $S$  [1].

Our second aim is to clarify which of the two NH groups of Cs is the origin of an apparent additional signal detectable in the aromatic section of  $^1\text{H}$  NMR spectra from intact m. gastrocnemius. The unexpected visibility of an amide group may be used to obtain information about possible sites of interaction with macromolecules by means of hydrogen-bond formation.

## 2. Theory

Residual dipolar coupling is a well-known effect in the (P)Cr methylene doublet in human muscle tissue in vivo and the corresponding Eq. (1) adequately describes the detectable line splitting (as a function of  $\theta$ ) for the interaction of two isochronous protons. Using the known value of  $SD_0 = 4.92$  Hz [1], Eq. (1) is employed in the present paper to determine the muscle fibre orientation within the acquisition volume by means of the splitting of the (P)Cr doublet. Moreover, the orientation dependence of the Tau- $\text{CH}_2$  signal is evaluated via the same Eq. (1).

Molecular mobility of the  $\text{CH}_3$  group has to be treated differently, because in general the possible spectral pattern of this spin system is by no means trivial. Its common model is a rotor with  $C_3$  symmetry. The transitions of this system with total spin  $3/2$  are known from solid-state NMR [10]. Regarding the plane of the equilateral triangle formed by the three protons, the spectrum depends on the orientation of the normal vector of this plane with respect to  $\vec{B}_0$ . Denoting the angle between these two vectors by  $\psi$  and neglecting rotation at first, the components of the  $\text{CH}_3$  signal are three dou-

plets and one singlet. The transition frequencies of the doublets depend on  $\psi$ .

Taking rotation into account, the characteristic angle is the orientation  $\eta$  of the axis of rotation with respect to  $\vec{B}_0$ . In general, methyl groups rotate around the C–R axis which is perpendicular to the plane of the triangle (Fig. 1). The corresponding energy corrections were calculated by Andrew and Bersohn, the result is a simplification of the spectra: a triplet with intensity ratios 1:2:1 can be observed (Fig. 1). In contrast to Eq. (1) the line splitting of the entire triplet (between the outer satellites!) is:

$$\Delta\nu_{\text{CH}_3} = \frac{3}{2}D_0(3\cos^2\eta - 1). \quad (2)$$

Molecular libration has to be respected since even the line splitting of the methylene group of acetonitrile trapped in an organic crystal at  $T = 216$  K significantly deviates from the value of  $3D_0 = 63.9$  kHz which is expected in the case of freezing of any type of motion [11]. For adapting this relation to methyl groups in cytosolic metabolites *in vivo* we assume that the C–R axis undergoes a tumbling motion similar to that of the internuclear vector between the protons of the  $\text{CH}_2$  group. Accordingly, the order parameter  $S$  for this 3-spin system can be introduced by

$$\Delta\nu_{\text{CH}_3} = \frac{3}{2}SD_0(3\cos^2\eta - 1). \quad (3)$$

In general, distinction between the preferred orientations  $\theta$  of a  $\text{CH}_2$  group and  $\eta$  of a  $\text{CH}_3$  rotor in (P)Cr is requested. Only if the break in reorientation symmetry of the different spin systems has the same origin, a uniform “director” forces the non-vanishing of the dipolar line splitting and both orientation dependences coincide.

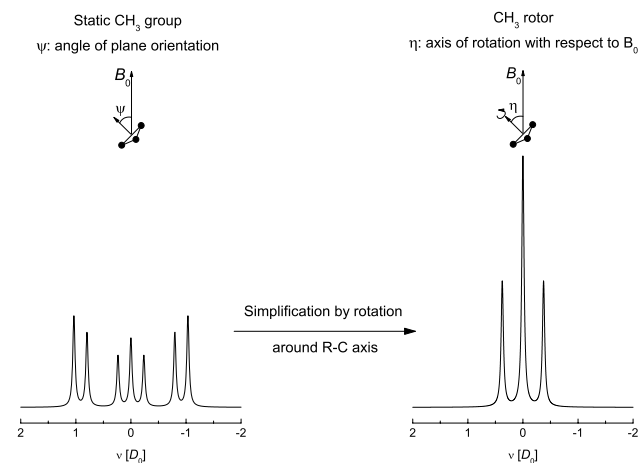


Fig. 1. Effect of rotation of a methyl group (triangular configuration) around the R–C axis of an organic molecule on the spectrum of three dipolar-coupled protons [10]. The seven resonances of the static  $\text{CH}_3$  group (left) collapse into a triplet (right) whose line splitting depends on the orientation of the axis of rotation (which is perpendicular on the plane of the three protons) with respect to  $\vec{B}_0$ .

In distinct contrast to the coupling of isochronous spins, the interaction of the imidazole ring protons of Cs produces second-order spectra at 1.5 T [2]. The observable coupling strength,  $Sk$ , combined with the chemical shift difference of the H2 and H4 protons (resonating at  $\delta \approx 8$  and 7 ppm) yields Clebsch–Gordan coefficients that characterize the system of dipolar-coupled protons. Like the atomic hydrogen (electron–proton) hyperfine interaction, its energy levels are given by a Breit–Rabi formula which contains additional terms that cause asymmetric line positions. These corrections were used to define an asymmetry parameter  $A_P$  in [2]. Fig. 2 illustrates the origin of this asymmetry by means of a Breit–Rabi diagram. In the regime of the Paschen–Back effect, i.e., for weak couplings (large Breit–Rabi parameters  $x = 2h\delta/(Sk)$ ;  $\delta =$  chemical shift difference in Hz), the energies of the eigenstates  $\psi_2$  and  $\psi_3$  depend linearly on  $x$ . For strong couplings (small  $x$  values), the deviation from this asymptotic behaviour increases and one doublet is shifted upfield while the other is shifted downfield.

Additionally, the line intensities also change owing to terms weighted by Clebsch–Gordan coefficients. However, because of the limited spectral resolution and the presence of a large Cs pool which is not affected by line splitting [2], only the asymmetric line positions can be exploited in the case of the imidazole ring protons (for the following, see [2]). The asymmetry parameter

$$A_P = -h\delta\sin^2\alpha + \frac{Sk}{2}\sin\alpha\cos\alpha \quad (4)$$

can be determined by spectral analysis and yields the rotational angle  $\alpha$  (compared to [2], here the chemical shift difference is denoted  $\delta$ ). This source of information allows access to the coupling strength  $Sk$ , and thus even-

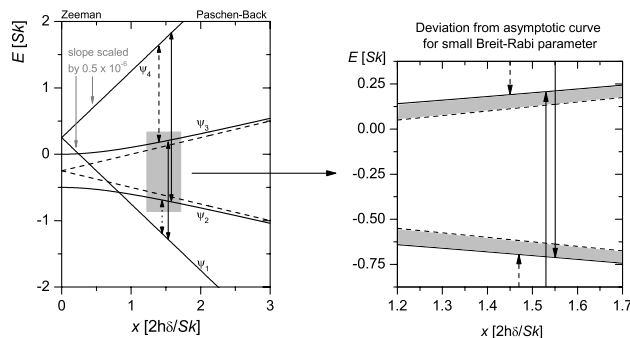


Fig. 2. Breit–Rabi diagram illustrating the origin of the asymmetry quantified by the parameter  $A_P$ . The area in grey (left) is magnified (right) to show the increasing deviation of the energy function of spin states  $\psi_2$  and  $\psi_3$  from the asymptotic linear shape (---), when the Breit–Rabi parameter  $x = 2h\delta/(Sk)$  decreases. Transitions that induce the X1,X2 and X3,X4 doublets of Cs are indicated by solid and dashed arrows. The former increase, the latter decrease, leading to asymmetric shifts of the doublets. The slope of the energy functions of eigenstates not affected by the mixing angle  $\alpha$  is scaled down by the factor  $0.5 \times 10^{-6}$ .

tually the order parameter  $S$ , alternatively to the line splitting. The procedure is as follows: The angle  $\alpha$  appears in the rotation matrix which tilts the two-dimensional Hilbert subspace  $\{|m, m'\rangle\}$  with  $m + m' = 0$  for an appropriate eigenbase of the system;  $\alpha$  depends on the ratio of the coupling strength  $Sk$  and the chemical-shift difference  $\delta$  of the coupled spins:

$$\tan 2\alpha = \frac{Sk}{2h\delta} = x^{-1}. \quad (5)$$

We use the first equality to eliminate  $Sk$  in Eq. (4)

$$A_P(\alpha) = h\delta\left(\frac{1}{2}\tan 2\alpha \sin 2\alpha - \sin^2\alpha\right) = -\frac{h\delta}{2}\left(1 - \frac{1}{\cos 2\alpha}\right),$$

which allows  $\alpha$  to be expressed by the observable quantities  $A_P$  and  $\delta$ :

$$\alpha = \frac{1}{2} \arccos \frac{\delta}{(2A_P/h) + \delta}. \quad (6)$$

The angle from Eq. (6) is finally inserted into Eq. (5) to obtain the measurable coupling strength as a function of the asymmetry parameter:

$$Sk/h = 2\delta \tan 2\alpha(A_P, \delta). \quad (7)$$

The experimentally observed coupling strength  $Sk/h$  compared with  $D_0$  (calculated on the basis of the geometry of the molecule) after correction of the orientation dependence in  $k$  eventually yields the order parameter  $S$ .

Details of the molecular mobility cannot be derived with this approach. However, from *in vivo* MRS data of the three endogenous metabolites (P)Cr, Tau, and Cs we may infer significant *differences* in molecular dynamics. The chemical structures of these metabolites (Fig. 3) suggest a much weaker interaction between the two imidazole ring protons because of their longer distance compared to the distance of the protons within the (P)Cr or Tau methylene groups. This is true if the motional restrictions are of the same magnitude for these metabolites.

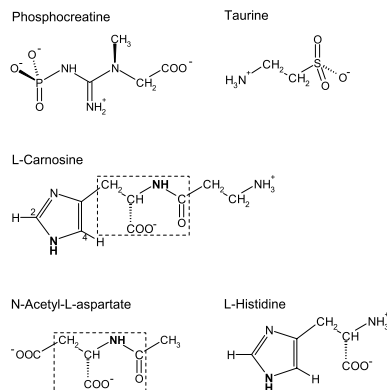


Fig. 3. Chemical structures of phosphocreatine (PCr), taurine (Tau), L-carnosine ( $\beta$ -alanine-L-histidine; Cs), *N*-acetyl-L-aspartate (NAA), and L-histidine (His). The common core of Cs and NAA is indicated by dashed boxes, NH groups studied in detail are indicated in bold.

A study of restricted motion of intracellular metabolites must also include the identification of possible sites of interaction. In [2] we already pointed out the striking difference between the signal intensities of H2 and H4 in m. gastrocnemius *in vivo* and speculated on hydrogen-bond formation of one of the two NH groups of Cs with a larger structure. This effect would slow down chemical exchange making one extra proton detectable. In previous studies [12,13], an additional signal component at  $\delta \approx 8$  ppm was indeed identified, but could not be assigned unambiguously to an amide group. To clarify this point,  $^1\text{H}$  NMR spectra of *N*-acetyl-L-aspartate (NAA) and L-histidine (His) in aqueous solutions were analysed. His is one of the two constituents of Cs and was chosen to study interactions of the isolated imidazole-NH. The NAA molecule has the same “core” as Cs (Fig. 3) and is therefore a good candidate for dedicated studies of interactions of the amide group of the peptide bond. Reduced chemical exchange *in vitro* is achieved by increasing the acidity of the model solutions. Comparison with the spectra of Cs reveals the nitrogen at the site with the smaller proton exchange rate [14] which therefore represents a possible site for macromolecular interaction.

### 3. Experimental

#### 3.1. MR tomograph

All experiments were performed on a clinical whole-body MR scanner with  $B_0 = 1.5$  T (MAGNETOM Vision Plus with Helicon 2E magnet; Siemens AG, Erlangen, Germany). The employed antenna systems are standard equipment as are the pulse sequences for MRI and the software for evaluation of the data (LUISE; Siemens). In the *in vivo*  $^1\text{H}$  NMR experiments, spins were excited via the body resonator and the signal was detected with the flexible extremity coil ( $17 \times 37$  cm<sup>2</sup>) wrapped around the calf of the volunteer. The standard head coil was used in the experiments with model solutions. For MRS measurements standard sequences with modified water and fat suppression techniques were employed.

#### 3.2. *In vivo* NMR spectroscopy

Data of five male healthy volunteers (age: 19–27 years) were evaluated in this study. Informed consent according to procedures approved by the Institutional Review Board was obtained from all volunteers prior to each examination, after the nature of the procedures had been fully explained. Evaluated datasets were already obtained in the context of [2]. However, in the present study different aspects are considered. For the sake of completeness, the procedure of measurement is shortly described:



Placement of the MRS voxel of  $(2\text{ cm})^3$  within m. gastrocnemius was preceded by acquisition of three orthogonal images of the calf. The orientation of the muscle fibres (“pennation angle”  $\theta$ ) with respect to the direction of the magnetic field was estimated by means of the line splitting of the (P)Cr doublet (procedure according to [2]). With knowledge of the precise orientation dependence of this line splitting determined in [1], this method indeed permits reliable determination of the fibre orientation which is not directly accessible by means of MR imaging. A linewidth  $\Delta\nu_{1/2}({}^1\text{H}) \approx 18\text{ Hz}$  of the tissue water signal was achieved with volume-selective shim.

Although the concentration of Cs is up to 20 mM in human muscle tissue [15] the NMR-detectable signal of this metabolite in human calf muscle is very weak and short-*TE* acquisition is required to minimize loss of signal. Localized  ${}^1\text{H}$  NMR spectra were obtained with a stimulated echo acquisition mode (STEAM) sequence with minimum *TE* = 10 ms, middle interval *TM* = 15 ms, *TR* = 2 s, and 500 excitations. Two 25.6-ms Gaussian-shaped CHESS pulses, centered at  $\delta = 4.7\text{ ppm}$  and  $\delta = 1.4\text{ ppm}$ , followed by spoiler gradients afforded efficient water and lipid signal suppression, respectively. The volunteers were able to keep the leg calm during the measurement time of 16.7 min.

### 3.3. MRS of model solutions

Aqueous model solutions of carnosine, NAA, and histidine (50 mM each; all compounds purchased from Sigma–Aldrich Chemie GmbH; Steinheim, Germany) were prepared to study the aromatic region of  ${}^1\text{H}$  NMR spectra at different pH. 1 M HCl was added to the solutions to detect the NH groups. Spectra were compared with in vivo data to identify the origin of a putative additional signal resonating at 8 ppm. The experiments were performed with the standard STEAM sequence of the scanner (*TE* = 10 ms, middle interval *TM* = 15 ms, *TR* = 2 s, 256 excitations,  $\text{VOI} = (2\text{ cm})^3$ , single water-signal-suppression pulse).

### 3.4. Data processing and analysis

Postprocessing of free induction decays (FID) included zero-filling to 4 k complex data points, linebroadening (by multiplication with a Gaussian function), and Fourier transformation, followed by phase correction and baseline flattening (by subtraction of a spline fit). The resulting Fourier spectra were analysed by means of least-squares fits assuming Gaussian line-shapes of the resonances.

Finally, Origin 6.1 (OriginLab, Northampton, MA, USA) was employed to display the data and to determine orientation dependence of line splittings (Eqs. (1) and (3)). Coupling constants for (P)Cr, Tau, and Cs were calculated on the basis of geometric data obtained

by means of ISIS/Draw 2.3 (MDL Information Systems, San Leandro, CA, USA) and ACD/3D 4.52 (Advanced Chemistry Development, Toronto, Canada). This software was also used to display the structure of a carnosylated phospholipid.

## 4. Results

### 4.1. In vivo MRS experiments

Fig. 4 shows the regions of in vivo  ${}^1\text{H}$  NMR spectra of human m. gastrocnemius which exhibit effects of residual dipolar couplings. The involved metabolites are (P)Cr (methylene doublet at  $\delta = 3.93\text{ ppm}$  and methyl triplet at  $\delta = 3.03\text{ ppm}$ ), Tau (methylene doublet at  $\delta = 3.34\text{ ppm}$ , one peak overlaps with the Cho signal) and a pool of Cs with motional restriction giving rise to the aromatic resonances X1–X4. Regarding their positions relative to the unsplit signals of H2 ( $\delta \approx 8\text{ ppm}$ ) and H4 ( $\delta \approx 7\text{ ppm}$ ) of Cs molecules which are not subjected to dipolar line splitting, the doublets X1, X2 and X3, X4 are shifted down- and upfield, respectively. This simplifies the identification of the connectivity between the imidazole ring protons H2 and H4 [2]. An additional signal which overlaps with the H2 resonance will be assigned to one of the NH protons of Cs (see below).

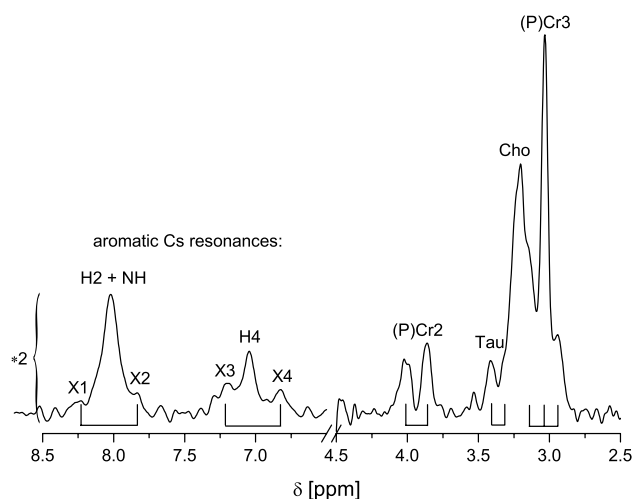


Fig. 4. Localized in vivo 1.5-T  ${}^1\text{H}$  NMR spectrum of m. gastrocnemius of a 19-year-old volunteer. The resonances X1–X4 show asymmetries in line positions characteristic for second-order spectra [2]. Compared to creatine/phosphocreatine ((P)Cr) and taurine (Tau) the restriction of molecular mobility of carnosine (Cs) appears to be stronger as suggested by the larger dipolar line splitting of the Cs imidazole protons although their internuclear distance is larger than that of the dipolar-coupled protons in (P)Cr and Tau. The intensities in the aromatic region are magnified by a factor of 2 and the centre of the apodization filter is shifted by 200 ms to enhance resolution (compared to Fig. 7 in [2], the Cs concentration appears to be higher for this volunteer; actually we have no explanation for this discrepancy). Experimental technique: STEAM with *TR* = 2 s, *TE* = 20 ms, *TM* = 15 ms, NEX = 500, voxel size =  $(2\text{ cm})^3$ .

The dipolar line splitting of X1, X2 and X3, X4 exceeds the splitting of the (P)Cr and Tau signals, although the internuclear distance of the imidazole ring protons is much larger than that within the methylene or methyl group (0.425 vs. 0.178 nm). This is remarkable and indicates already that the order parameters differ significantly.

Because of partial overlap with the intense choline singlet (Cho,  $\delta = 3.2$  ppm), the fine structure of the (P)Cr methyl triplet and of the Tau methylene doublet could not be evaluated directly. The splitting of the triplet was therefore estimated from the chemical shift difference between the centre peak at  $\delta \approx 3.03$  ppm and the satellite at the high-field side, while the Tau splitting was taken as twice the distance between the signal at  $\delta \approx 3.4$  ppm and the dip between this peak and the Cho resonance. Since the upfield component of this doublet is superimposed by the Cho signal, this method should yield a lower bound for the splitting; altogether, this value is less reliable than the result of the evaluation of the triplet. In one spectrum of the series, however, the resolution was sufficiently high to enable a fit of all 6 resonances (Fig. 5).

Table 1 shows the results for the (P)Cr triplet from five volunteer examinations. To check for a possible correlation between the angles  $\eta$  and  $\theta$ , the line splittings are plotted as a function of the orientation derived from the  $\theta$ -dependence of the methylene doublet splitting (Fig. 6). The data indicate  $\theta \approx \eta$  (a simultaneous collapse of the multiplets for the magic angle  $\theta \approx 55^\circ$  was already reported in [6]), which confirms Eq. (3) qualitatively and yields  $SD_0 = (6.0 \pm 0.4)$  Hz.

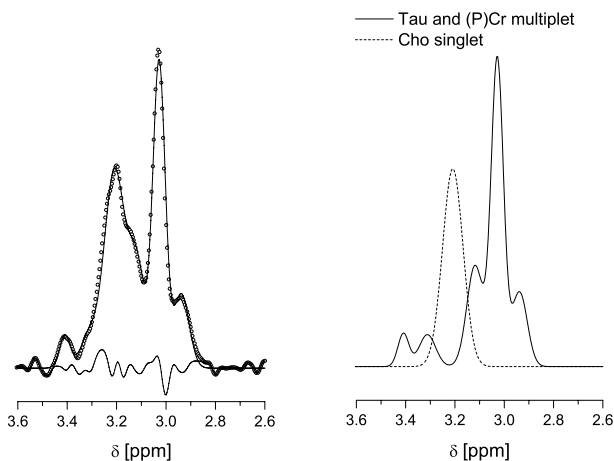


Fig. 5. Analysis of the choline (Cho) region of the localized in vivo  $^1\text{H}$  NMR spectrum in Fig. 4. Assuming six resonances (right) for the singlet of Cho trimethylamine, doublet of taurine (Tau) methylene, and triplet of creatine/phosphocreatine ((P)Cr) methyl protons, the observed spectrum ( $\circ$ ) can be well approximated by a superposition of Gaussian line shapes (left; the residual signal is also drawn). The fit yields line splittings  $\Delta\nu = 6.7$  Hz for Tau- $\text{CH}_2$  and  $\Delta\nu = 11.4$  Hz for (P)Cr- $\text{CH}_3$ .

Table 1

Line splitting  $\Delta\nu$  of methylene triplet of creatine/phosphocreatine ((P)Cr) in  $^1\text{H}$  NMR spectra of human m. gastrocnemius in vivo at the corresponding fibre orientation  $\eta$

Study #	$\delta$ (P)Cr3 [Hz]	$\delta$ sat [Hz]	$\Delta\nu$ [Hz]	$\eta$ [°]
1	194.0	188.1	11.8	27.0
2	190.6	182.3	16.6	14.4
3	191.4	183.4	16.0	8.3
4	192.8	183.9	17.8	0.0
5	195.6	187.9	15.4	20.7

Note.  $\Delta\nu$  = twice the frequency difference (peak-to-peak) of the centre line at  $\delta = 3.03$  ppm and the high-field satellite (sat). Chemical shift reference: tetramethylsilane (TMS),  $\delta = 0.0$  ppm.

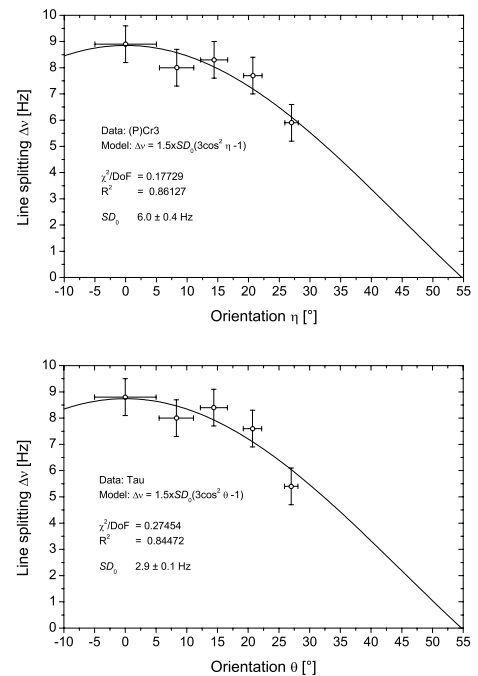


Fig. 6. Residual dipolar line splittings as a function of orientation: Values of the pennation angle  $\theta$  determined from the (P)Cr doublet were used to test for possible analogous description of the orientation dependence of (P)Cr triplet (top) and Tau doublet (bottom) from localized in vivo  $^1\text{H}$  NMR spectra of human m. gastrocnemius. Data indicate that a common director for the  $\text{CH}_3$  and the  $\text{CH}_2$  spin systems can be assumed thus enabling the characterization of the detectable preferred orientation of the C-R axis ( $\eta$ ) and  $\langle \vec{r}_{ij} \rangle(\theta)$  by the pennation angle of the muscle fibre (note even the similar deviations of the data points from the fit). The error bars for  $\theta$  refer to Eq. (1) applied to the (P)Cr doublet (for details, see [2]) and are therefore identical in both plots just as the uncertainty in frequency which was taken from the spectral resolution of  $\pm 0.7$  Hz.

Table 2 gives line splittings for Tau from five studies. With Eq. (1) we obtain  $SD_0 = (2.9 \pm 0.1)$  Hz for this metabolite (Fig. 6). Both fits indicate that the time average of the C-R axis of the  $\text{CH}_3$  group as well as the preferred orientation of  $\langle \vec{r}_{ij} \rangle$  of the Tau- $\text{CH}_2$  protons can be characterized approximately by the pennation angle. This is reasonable because the macroscopic anisotropic muscle structure is suspected to cause restrictions in reorientations (see Section 5).

Table 2  
Line splitting  $\Delta\nu$  of taurine (Tau) doublet in  $^1\text{H}$  NMR spectra of human m. gastrocnemius in vivo at the corresponding fibre orientation  $\theta$

Study #	$\delta$ Tau [Hz]	$\delta$ dip [Hz]	$\Delta\nu$ [Hz]	$\theta$ [°]
1	215.5	212.8	5.4	27.0
2	216.8	212.6	8.4	14.4
3	216.9	212.9	8.0	8.3
4	219.8	215.4	8.8	0.0
5	221.0	217.2	7.6	20.7

Note.  $\Delta\nu$  = twice the frequency difference of the resolved Tau signal at  $\delta \approx 3.4$  ppm and the dip between this peak and the Cho resonance. Chemical shift reference: tetramethylsilane (TMS),  $\delta = 0.0$  ppm.

Table 3

Asymmetry parameter ( $A_P$ ), frequency difference of coupled spins ( $\delta$ ), rotational angle ( $\alpha$ ), and observed coupling strength ( $Sk/h$ ) of imidazole ring protons of carnosine (Cs) at the corresponding fibre orientation  $\theta$

Study #	$A_P$ [ppm]	$\delta$ [ppm]	$\alpha$ [°]	$Sk/h$ [ppm]	$\theta$ [°]
1	0.01	0.983	5.73	0.40	27.0
2	0.03	0.960	9.87	0.69	14.4
3	0.05	0.960	12.54	0.90	8.3
4	0.02	0.900	8.39	0.54	0.0
5	0.01	0.945	5.84	0.39	20.7

Note.  $\delta$  = frequency difference of unsplit H2 and H4 resonances;  $\alpha$  calculated from  $A_P$  with use of Eq. (6); precision of measurement of line positions: 0.004 ppm; derived quantities approximated to 2 digits.

Analysis of line splittings led to a dipolar coupling constant of  $SD_0 = (17.7 \pm 0.3)$  Hz for the imidazole ring protons in Cs [2]. The spectra we obtained previously were now evaluated on the basis of second-order effects as implied by Eq. (7). Table 3 gives the asymmetry parameter  $A_P$  (average of two values each for X1,X2 and X3,X4 doublets), the chemical shift difference  $\delta$  of H2 and H4 protons, the rotation angle  $\alpha$  Eq. (6), and  $Sk/h$  Eq. (7) from five studies with different pennation angles  $\theta$ . The fit of  $Sk/h$  as a function of  $\theta$  (Fig. 7) using the relation

$$Sk/h = SD_0(3\cos^2\theta - 1) \quad (8)$$

for anisochronous spins [2] yields  $SD_0 = (21.5 \pm 2.7)$  Hz, which is larger than the coupling constant derived from the X1, X2 and X3, X4 splittings.

The predictions for the coupling parameters  $D_0$  of (P)Cr and Tau methylene, (P)Cr methyl, and Cs imidazole ring protons are listed in Table 4. They are compared to the observed values determined by means of line splitting (all spin systems), phase modulation/zero-quantum evolution ( $\text{CH}_2$  of (P)Cr, see also [16]) or asymmetry parameters (H2–H4 of Cs). Regarding the different types of spin systems, the appropriate relation between the detectable coupling strength  $\Delta\nu = Sk/h$  and the coupling constant  $D_0 = \frac{\mu_0(\gamma h)^2}{4\pi h r^3}$ , i.e., Eqs. (1), (3), and (8), respectively, must be employed to derive  $S$ . Since the dipolar interaction strongly depends on the internuclear distance  $r$ , the line splitting of Cs expected from theory

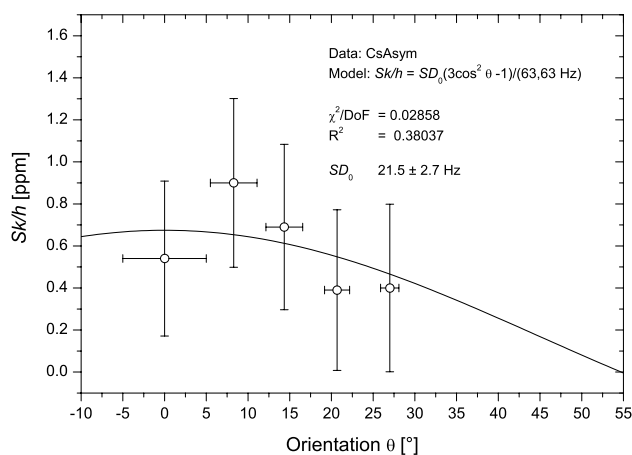


Fig. 7. Residual dipolar coupling strength of carnosine (Cs) as a function of orientation (pennation angle  $\theta$ ) derived from asymmetries of Cs resonances in localized in vivo  $^1\text{H}$  NMR spectra of human m. gastrocnemius. The large error bars are caused by the slope of the tan in Eq. (7).

Table 4

Internuclear distances ( $r_{\text{HH}}$ ), expected ( $D_0$ ), and observed dipolar coupling constant ( $D_{\text{obs}}$ ), and order parameter ( $S$ ) for imidazole ring protons in carnosine (Cs), the methylene and methyl protons in creatine/phosphocreatine ((P)Cr) and methylene protons in taurine (Tau)

Connectivity	$r_{\text{HH}}$ [nm]	$D_0$ [kHz]	$D_{\text{obs}}$ [Hz]	$S$ [ $10^{-4}$ ]
H2–H4 in Cs	0.425	1.564	$17.7 \pm 0.3^a$	$113 \pm 2$
			$21.5 \pm 2.7^b$	$137 \pm 17$
$\text{CH}_2$ in (P)Cr	0.178	21.294	$6.3 \pm 0.1^c$	$3.0 \pm 0.1$
			$4.92^d$	2.3
			$5.56^e$	2.6
$\text{CH}_3$ in (P)Cr	0.178	21.294	$1.5 \pm 0.1^a$	$2.8 \pm 0.05$
$\text{CH}_2$ in Tau	0.178	21.294	$2.9 \pm 0.1^a$	$1.4 \pm 0.1$

Note. Applied measurement techniques for  $D_{\text{obs}}$ :

<sup>a</sup> Line splitting.

<sup>b</sup> Asymmetries.

<sup>c</sup> Phase modulation (see also [16]).

<sup>d</sup> Line splitting from [1].

<sup>e</sup> Zero-quantum evolution period of ca. 120 ms reported in [6], corresponds to a line splitting of 16.7 Hz.

is much smaller than that of (P)Cr or Tau with the remarkable consequence that the order parameter of Cs is by far the highest one: the order of magnitude is  $10^{-2}$  vs.  $10^{-4}$  (Table 4). For spin systems which allowed more than one independent approach to determine  $S$  (two for H2–H4 of Cs, three for  $\text{CH}_2$  of (P)Cr), consistent values were obtained by the different methods.

#### 4.2. MRS of model solutions

Fig. 8 shows a series of  $^1\text{H}$  NMR spectra of Cs model solutions with different pH in the range of 1.1–7.1. Increasing acidity uncovers the anticipated signal at  $\delta \approx 8$  ppm which coincides with the H2 resonance at

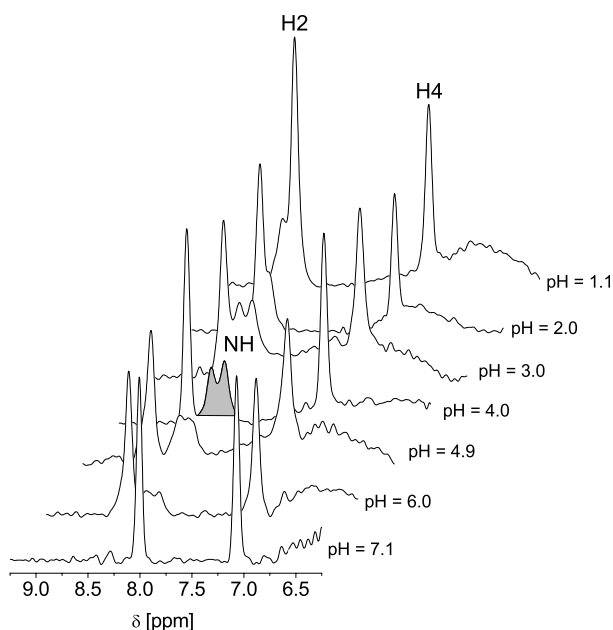


Fig. 8. Aromatic resonances of 1.5-T  $^1\text{H}$  NMR spectra of Cs aqueous solutions (50 mM) at different pH. When acidity increases a doublet signal with pH-dependent chemical shift becomes visible at the high-field side of the H2 resonance (grey area). A broad resonance at the high-field side of the H4 signal is attributed to fast exchangeable protons ( $-\text{NH}_3^+$ ). Experimental technique: STEAM with  $TR = 2$  s,  $TE = 20$  ms,  $TM = 15$  ms,  $NEX = 256$ , voxel size =  $(2 \text{ cm})^3$ .

physiological pH in vivo ( $\text{pH} = 7.1$ ) and which appears as a doublet with pH-independent splitting corresponding to a scalar coupling constant  $J = (7.6 \pm 0.4)$  Hz. The line positions of H2, H4, and of the doublet shift when pH changes.

For comparison, Fig. 9 displays series of  $^1\text{H}$  NMR spectra of NAA and His model solutions, respectively,

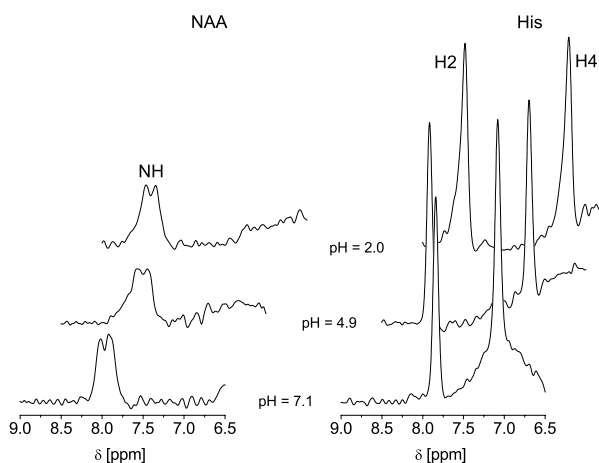


Fig. 9. Aromatic resonances of 1.5-T  $^1\text{H}$  NMR spectra of NAA (left) and His (right) aqueous solutions (50 mM) at different pH assigned to the amide proton (NAA) and ring protons at positions 2 and 4 (His). When acidity increases a down-field shift is observed in both cases. Experimental technique: STEAM with  $TR = 2$  s,  $TE = 20$  ms,  $TM = 15$  ms,  $NEX = 256$ , voxel size =  $(2 \text{ cm})^3$ .

with pH in the range of 2.0–7.1. NAA spectra show a scalar-coupled doublet at  $\delta \approx 8$  ppm assigned to the amide proton whose coupling constant of the interaction with the methine proton is  $J = (7.1 \pm 0.4)$  Hz. The signal is broadened owing to chemical exchange, but is already intense for neutral solutions. Like the doublet seen in the Cs spectra (Fig. 8), it undergoes a downfield shift when the acidity of the solution increases.

The experiment with His solutions could exclude the imidazole NH proton as possible origin of the doublet resolved in some of the spectra in Fig. 8. Only chemical shifts changed upon variation of pH, no additional signal was seen at  $\delta \approx 8$  ppm. The broad signal under the H4 resonance is assigned to the terminal  $\text{NH}_3$  group of His (Fig. 9).

## 5. Discussion

Evaluation of order parameters of endogenous metabolites in human m. gastrocnemius derived from residual dipolar couplings in localized in vivo  $^1\text{H}$  NMR spectra indicate significant differences in molecular mobility. While absolute values cannot be obtained with the technique employed here, the data still permit a qualitative assessment of the mobility of creatine and phosphocreatine, taurine, and carnosine in intact human muscle tissue. It is also important to note that all parameters related to the pennation angle are afflicted with a certain averaging because fibre orientation varies within a few centimeters in m. gastrocnemius. However, this study focused on spectra of this muscle because it is easy to measure with single-voxel  $^1\text{H}$  MRS (e.g., compared to m. tibialis anterior) and comparative statements are reliable.

Because non-vanishing residual dipolar couplings are attributed to restrictions in molecular reorientation as a consequence of interactions with the anisotropic muscle structure, the fibre direction is the only detectable preferred orientation. It determines  $\langle \vec{r}_{ij} \rangle$  of the two-spin systems and the remaining alignment of the  $\text{CH}_3$ -rotor axis. In our related paper in this issue, which deals with the details of the (P)Cr- $\text{CH}_2$  phase modulation [16], the justification for direct use of the pennation angle as the parameter for the orientation-dependent relations (without an Euler transformation) is also discussed. The obtained value of the observable coupling constant  $SD_0 = (6.3 \pm 0.1)$  Hz is therefore appropriate to derive an order parameter for comparison with other spin systems.

The resulting value  $S \approx 3 \times 10^{-4}$  indicates that the dipolar interaction in (P)Cr is scaled down very effectively either by motion of the entire molecule or by intramolecular reorientation of the methylene group. Both processes enable averaging of intermolecular dipolar interactions which leads to well-resolved resonance



lines in contrast to spectral patterns known from solid-state NMR.

But hindered reorientation of methylene is not the whole story, since a residual dipolar coupling also affects the methyl group of this metabolite. Hence by *in vivo*  $^1\text{H}$  MRS, we obtain information about the mobility of this section of the molecule (Fig. 3). Alonso et al. [13] observed a connectivity between these two subgroups in 2D HOHAHA experiments on intact frog m. gastrocnemius, which proves additionally that both subgroups are restricted in mobility. The experiments on human calf muscle demonstrate that the interaction of the protons *within* each group is the dominant one owing to the strong spatial dependence of the direct spin–spin coupling. Otherwise, a significant  $\text{CH}_2$ – $\text{CH}_3$  interaction would lead to higher multiplicities, i.e., further splittings of the doublet and the triplet.

The similarity of the orientation dependence of the dipolar-coupling effects of (P)Cr triplet and Tau doublet is remarkable (Fig. 6). It agrees perfectly with data for the (P)Cr doublet published in [1] and even the scatter of the datasets is very similar: if the splitting of the triplet decreases, that of the doublet follows. The plot of the doublet splitting vs. the triplet splitting yields a linear function with correlation coefficient  $R = 0.996$  (data not shown). This underlines the theory of a common director for all investigated spin systems so far. Our quantitative analysis of these dipolar-coupled spin systems therefore confirms the observation that all dipolar line splittings vanish simultaneously when the pennation angle  $\theta$  approximates the magic angle [6]. We conclude that the muscle structure determines the congruent symmetry break in reorientation of the  $\text{CH}_3$  rotor axis and the  $\text{CH}_2$  internuclear vectors ( $\vec{r}_{ij}$ ) of (P)Cr and Tau. This model also agrees with results obtained for lactate [3]. Only one common preferred direction is detectable for these systems and a uniform model of *in vivo* fixation of these metabolites has to be developed.

In distinct contrast to the order parameter obtained for the aliphatic groups, the parameter for the connectivity H2–H4 in carnosine is significantly larger. Both the line splitting and the asymmetry parameter yield  $S > 110 \times 10^{-4}$  (Table 4), which indicates a much more effective fixation of the molecule or at least of its imidazole ring within subcellular structures in the tissue. Yet,  $S$  can only be related to the degree of motional averaging and gives no absolute measure for immobilization. Therefore, it is not possible to indicate common parameters like binding constants, etc. at this stage.

Use of the asymmetric line positions involves a larger uncertainty of  $S$  because of the characteristics of second-order spectra discussed in [2]:  $A_P$  is not very sensitive to increasing state mixing quantified by  $\alpha$  in Eq. (4). This is also illustrated in Fig. 2 (graph on the right) where the gap between the true eigenvalues and the linear asymptotes does not change substantially when  $x$  decreases.

Assuming an uncertainty of 0.01 ppm for the line positions and the derived parameter  $A_P/h$ , the error of the mixing angle  $\alpha$  calculated with Eq. (6) is about  $0.1^\circ$ . The crucial point is the steep slope of the tan function in Eq. (7): a small change of  $\alpha$  will result in large uncertainty of the coupling strength  $Sk/h$  (Fig. 7). Nevertheless, the value of  $SD_0$  obtained this way agrees with the line splitting reported previously [2] (Table 4). Data in Fig. 7 are insufficient to conclude that  $\langle \vec{r}_{ij} \rangle$  of this spin system obeys the same director as the others do (i.e., the fibre direction), but other studies indicate that this is indeed the case [2,9]. Yet a qualitative comparison of the order parameters should be possible.

Data in Table 4 demonstrate different molecular dynamics of the spin systems considered here. First, the aliphatic resonances indicate a relatively high mobility of  $\text{CH}_2$  and  $\text{CH}_3$  groups. In contrast to expectation, data show no significant difference of the mobility of C–R axis (which is oriented outwards and is suspected to perform faster reorientation) and the neighbouring  $\text{CH}_2$  group in (P)Cr (possibly an effect of the hydration shell in the region of the nucleophilic nitrogen that connects the two groups). Regarding molecular mass and possible rotations of the entire structures, taurine (125.1 amu; nearly linear configuration) should perform faster reorientation than PCr (209.1 amu; with larger mass off from the principal axes, Fig. 3). We thus expected—and found indeed—a smaller value of the order parameter  $S$  for Tau.

Second, the resonances of the H2–H4 system of carnosine (226.2 amu) reflect a large value of  $S$  for this metabolite. Because of the stiffness of the imidazole ring, the residual dipolar interaction will be effective if the ring is involved in intermolecular interactions (e.g., via the nucleophilic nitrogen  $\text{N}^1$ ).

Proton NMR spectra of the model solutions explain the higher signal intensity of the *in vivo* H2 resonance. The amide group of the peptide bond yields a resolved doublet (marked peak in Fig. 8) while the imidazole-NH cannot be detected, in agreement with the peak assignment given in [12]. The conclusions are as follows: The assignment “H2” of the *in vivo* resonance at  $\delta \approx 8$  ppm is incomplete, because it disregards the signal contribution of the amide proton. The doublet is broadened due to chemical exchange, therefore only an unresolved resonance is expected at 1.5 T *in vivo*. The distinct H2–H4 intensity difference indicates that the peptide-bond proton signal coincides with the H2 peak. Finally, the signal does not interfere with the satellites X1–X2, because their asymmetry (attributed to a direct H2–H4 interaction [2]) is the same as for the satellites X3–X4 of H4.

The experiments with the Cs model solutions demonstrated a strong pH-dependence of the intensity and the chemical shift of the peptide-bond proton (Fig. 8). We observed a resolved  $J$ -coupled doublet (indirect interac-

tion of NH and CH protons) for  $\text{pH} \leq 4.0$ , a broad peak for  $\text{pH} = 6.0$ , but no additional signal for  $\text{pH} = 7.1$  besides H2 and H4. These changes are explained by the pH-dependence of the rate of amide-proton chemical exchange [14]. Slow exchange rates at low pH enable high signal intensity, a narrow linewidth, and a resolved doublet structure, while fast exchange rates at higher pH are related to broad signals of low intensity.

Different degrees of protonation cannot explain the pH-dependence of the signal intensity because of  $\text{p}K_s \approx 15$  for an amide proton, thus even at neutral pH the nitrogen is completely protonated. They also cannot account for the different properties of the resonance of the amide proton in NAA (no pH-dependence of signal intensity; Fig. 9). The differences are attributed to a higher chemical exchange rate in the case of the Cs amide proton owing to intramolecular interaction with the imidazole ring.

The visibility of the amide proton signal at 8 ppm in vivo thus implies slow chemical exchange. Low pH as explanation of this effect is certainly excluded in vivo since the H2 and H4 resonances are not shifted downfield (which is the cause that the H2 and NH signal are not separated). On the other hand, small exchange rates are also associated with shielding of amide protons from surrounding water, which commonly results from hydrogen-bond interactions [17]. The larger order parameter of carnosine compared to that of creatine and taurine implies stronger motional restriction of the molecule consistent with hydrogen-bond formation of the amide proton of Cs to a larger (macromolecular) structure.

Regarding the cause of the observed residual dipolar couplings of intramyocellular metabolites, the intrinsic muscle structure must play a crucial role as demonstrated in HOHAHA experiments [13] where negative ROE cross peaks indicating temporal binding of Cs and (P)Cr could only be observed in intact tissue samples and not in muscle tissue extracts and model solutions. Constraints of the molecules between the highly ordered actin–myosin chains or attachment to macromolecules (which could themselves be ordered within the cells) were discussed first [6]. Orientation of charged metabolites along an electric field established within the myofilaments [18] was also proposed [3,19]. The observation that several biochemical compounds in living tissue are affected by residual dipolar couplings with a congruent breaking of reorientation symmetry indicates that a common principle is valid. However, particular aspects of Cs metabolism are interesting in this context.

While the satellite signals in the aromatic region of the Cs spectrum are assigned to molecules with restricted mobility [2], the dominant and unsplit resonances H2 and H4 originate from a pool of Cs with free tumbling motion. Previous experiments on striated skeletal muscle showed that the living frog muscle is per-

meable to only 30% of its total Cs content in contrast to dead tissue [20]. In vivo data therefore suggest at least two compartments (free and more or less immobile) for Cs. However, the existence of an intra- and extracellular pool as in the case of lactate [3] is unlikely, since the cell membrane is highly impermeable for the charged Cs molecule.

In vitro experiments using radiolabeled Cs showed an interaction of the dipeptide with proteins which previously underwent carbonylation with a reactive sugar—this process is called “carnosinylation” [21]. During cell aging, also phospholipids of cellular membranes are oxidized to produce carbonyl groups; the process ultimately ends with the destruction of the phospholipid via lipid oxidation [22]. Cs is assumed to prevent these molecules from this fate by reacting with the carbonyl group of the attached sugar [21]; the supposed molecular compound is shown in Fig. 10. Since the orientation of membranes like the sarcolemma and the sarcoplasmic reticula (SR) are directly related to the muscle fibre axis, this protective reaction of Cs could explain the observation of its immobilization in muscle via the orientation-dependent dipolar coupling.

Therefore, Fig. 10 supplements the model of Cs immobilization as follows: If the NH group of the peptide bond approaches the phosphate group of the phospholipid, a hydrogen bond can be formed. A simi-

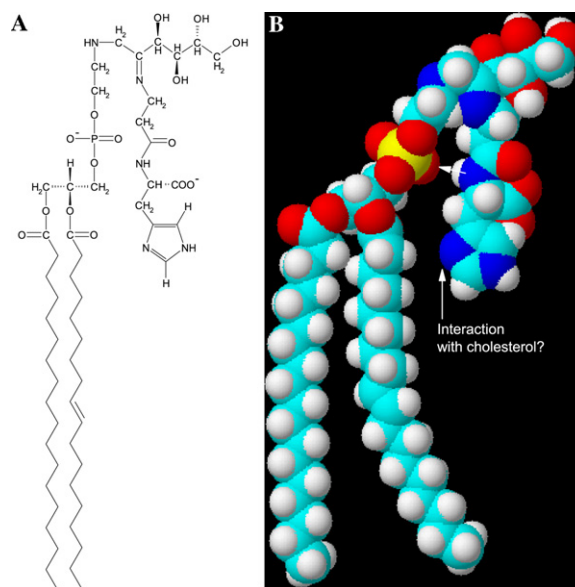


Fig. 10. Anticipated structure of a carnosinylated lipid (A). During cell aging, phosphatidylethanolamine reacts with a sugar and is carbonylated. This first step of glycation could be followed by a reaction of the sugar carbonyl group with the terminal amino group of Cs [21]. A 3D structure of the product of “carnosinylation” (B) illustrates possible hydrogen bond formation between the NH group of the peptide bond and the phosphate group of the lipid (arrow). Furthermore, the nucleophilic nitrogen  $\text{N}^1$  could approach the membrane-stabilizing compound cholesterol enabling fixation of the Cs imidazole moiety.

lar interaction is known from the membrane-stabilizing compound cholesterol whose hydroxyl group attaches to the carbonyls of the fatty acids [23]. Another site for fixation can arise from the nucleophilic nitrogen N<sup>1</sup> of the Cs imidazole ring. According to Fig. 10 the N<sup>1</sup> is oriented towards the inner part of the membrane (which is consistent with the observation that the aromatic groups of indole and aspirin, when interacting with phospholipids, are preferentially located close to the glycerol bridge [24]) and can therefore interact with the electrophilic hydroxyl group of cholesterol.

Likewise, taurine which is important for membrane stabilization in animal cells interacts with the sarcolemma. Restricted mobility of Tau in vivo is demonstrated by dipolar splitting resolved by line fitting in Fig. 5. Sebring et al. [25] showed that two Tau molecules can bind to phosphatidylcholine via interactions with the phosphate and the TMA residue, respectively.

Another possible site of Cs-membrane binding could arise from recent arguments regarding a crucial role of the metabolite in activation of Ca<sup>2+</sup>-release channels [26]. A temporal binding of Cs to the ryanodine receptor (or its immediate vicinity) on the SR membrane would explain the pool of Cs molecules with restricted mobility observed by means of <sup>1</sup>H NMR. Altogether, membrane phospholipids are likely to be involved in the phenomenon of residual dipolar couplings of small metabolites in living muscle tissue.

As discussed in [2], the H2 and H4 resonances observed in in vivo <sup>1</sup>H NMR spectra from m. gastrocnemius and m. soleus differ in line splittings (which is explicable by different fibre orientations) and relative intensity. The intensity difference of the two signals is less pronounced in m. soleus. Relaxation anisotropy must be considered here regarding the observation that the Cs resonances H2 and H4 are less broadened in m. soleus (spectra not shown). Because the fibre orientation in this muscle is close to the magic angle [5], dipolar relaxation terms which are determined by the common director are less effective in this case. A rotation of the structure or changeover from m. soleus to m. gastrocnemius would enable additional terms of relaxation, but the anisotropy should be identical for both resonances since the common director does not change. Hence, we prefer to attribute the difference in signal intensities to the reduced chemical exchange of the amide proton of the peptide bond (this exchange is possibly faster in m. soleus, resulting in a smaller signal at 8 ppm).

Carnosine is important for buffering pH during glycolysis (Cs and anserine contribute up to 40% to this effect [20]). Glycolysis is the prevalent energetic process (anaerobic) in “fast-twitch” fibres, the main component of m. gastrocnemius. In contrast, m. soleus consists mainly of “slow-twitch” fibres which gain energy from aerobic metabolism. This functional difference could im-

ply different types of fixation of Cs resulting in changes in <sup>1</sup>H NMR spectra which cannot be attributed to orientation-dependent effects.

To explain the origin of the different intensities of H2 and H4 resonances, Pan et al. [27] referred to the observation that carnosine in vivo forms various complexes with Cu<sup>2+</sup> [28] and proposed that the paramagnetic central ion accelerates T<sub>2</sub> relaxation of H2 and H4 differently. However, both signals vanish simultaneously if Cu<sup>2+</sup> ions are added in 1:100 dilution to the Cs solution [28]. Since the anticipated structures of the complexes do not indicate considerable differences of the relaxation rates, we believe that the different intensities of H2 and H4 can be explained by the signal contribution of the amide proton alone and not by complex formation.

The identification of residual dipolar couplings allowed the assignment of additional signals to intracellular compounds with restricted mobility. In the case of Cs, a connection between function and fixation can be suspected making high-resolution in vivo NMR spectroscopy a promising tool to explore the presently not fully understood biochemical function of this dipeptide (e.g., the significance of carnosinylation in the context of cell aging).

No attention has been paid so far to the aliphatic resonances ( $\delta \approx 3$  ppm) of Cs which are quite intense in <sup>1</sup>H NMR spectra of model solutions [2]. These peaks must be taken into account when the in vivo CH<sub>3</sub> resonances of (P)Cr, Cho, and Tau are quantified, unless further aspects of restricted mobility cause a significant reduction of these signals.

## Acknowledgments

We gratefully acknowledge the valuable support by Prof. Ulrich Haerberlen, Max-Planck-Institute for Medical Research, Heidelberg, and thank the ENC committee together with Suraj Manrao for generous support enabling L.S. the presentation of parts of this work at the 45th ENC.

## References

- [1] R. Kreis, C. Boesch, Liquid-crystal-like structures of human muscle demonstrated by in vivo observation of direct coupling in localized proton magnetic resonance spectroscopy, *J. Magn. Res. B* 104 (1994) 189–192.
- [2] L. Schröder, P. Bachert, Evidence for a dipolar-coupled AM system in carnosine in human calf muscle from in vivo <sup>1</sup>H NMR spectroscopy, *J. Magn. Res.* 164 (2003) 256–269.
- [3] I. Aslani, E. Shankland, T. Pratum, M. Kushmerick, Anisotropic orientation of lactate in skeletal muscle observed by dipolar coupling in <sup>1</sup>H NMR spectroscopy, *J. Magn. Res.* 139 (1999) 213–224.
- [4] H. Günther, *NMR-Spektroskopie*, Georg Thieme Verlag, Stuttgart, 1992.

- [5] P. Vermathen, C. Boesch, R. Kreis, Mapping fiber orientation in human muscle by proton MR spectroscopic imaging, *Magn. Res. Med.* 49 (2003) 424–432.
- [6] R. Kreis, C. Boesch, Spatially localized, one and two-dimensional NMR spectroscopy and in vivo application to human muscle, *J. Magn. Res. B* 113 (1996) 103–118.
- [7] R. Kreis, M. Koster, M. Kamber, H. Hoppeler, C. Boesch, Peak assignment in localized  $^1\text{H}$  MR spectra of human muscle based on oral creatine supplementation, *Magn. Res. Med.* 37 (1997) 159–163.
- [8] V. Ntziachristos, R. Kreis, C. Boesch, B. Quistorff, Dipolar resonance frequency shifts in  $^1\text{H}$  MR spectra of skeletal muscle: conformation in rats at 4.7 T in vivo and observation of changes postmortem, *Magn. Res. Med.* 38 (1997) 33–39.
- [9] R. Kreis, C. Boesch, Orientation dependence is the rule, not the exception in  $^1\text{H}$  MR spectra of skeletal muscle: the case of carnosine, *ISMRM Proc.* 8 (2000) 31.
- [10] E.R. Andrew, R. Bersohn, Nuclear magnetic resonance line shapes for a triangular configuration of nuclei, *J. Chem. Phys.* 18 (2) (1950) 159–161.
- [11] P. Gutsche, M. Rinsdorf, H. Zimmermann, H. Schmitt, U. Haeberlen, The shape and information content of high-field solid-state proton NMR spectra of methyl groups, *Solid State Nucl. Magn. Reson.* 25 (4) (2004) 227–240.
- [12] C. Arús, M. Bárány, Application of high field  $^1\text{H}$  NMR spectroscopy for the study of perfused amphibian and excised mammalian muscles, *Biochim. Biophys. Acta* 886 (1986) 411–424.
- [13] J. Alonso, C. Arús, W.M. Wrestler, J.L. Markley, Two-dimensional spectra of intact tissue: homonuclear Hartmann–Hahn spectroscopy provides increased sensitivity and information content as compared to COSY, *Magn. Res. Med.* 15 (1990) 142–151.
- [14] G.P. Connelly, Y. Bai, M.F. Jeng, S.W. Englander, Isotope effects in peptide group hydrogen exchange, *Proteins: Struct. Funct. Genet.* 17 (1993) 87–92.
- [15] R. Kohen, Y. Yamamoto, K.C. Cundy, B.N. Ames, Antioxidant activity of carnosine, homocarnosine, and anserine present in muscle and brain, *Proc. Natl. Acad. Sci. USA* 85 (1988) 3175–3179.
- [16] L. Schröder, Christian Schmitz, P. Bachert, Phase modulation in dipolar-coupled  $A_2$  spin systems: effect of maximum state mixing in  $^1\text{H}$  NMR in vivo, *J. Magn. Res.* 171 (2004) 207–212.
- [17] G. Wagner, Characterization of the distribution of internal motions in the basic pancreatic trypsin inhibitor using a large number of internal NMR probes, *Quart. Rev. Biophys.* 16 (1) (1983) 1–57.
- [18] G.F. Elliott, C.R. Worthington, How muscle may contract, *Biochim. Biophys. Acta* 1200 (1994) 109–116.
- [19] I. Asllani, E. Shankland, T. Pratum, M. Kushmerick, Effects of pH and molecular charge on dipolar coupling interactions of solutes in skeletal muscle observed by DQF  $^1\text{H}$  spectroscopy, *J. Magn. Res.* 163 (2003) 124–132.
- [20] C.L. Davey, The significance of carnosine and anserine in striated skeletal muscle, *Arch. Biochem. Biophys.* 89 (1960) 303–308.
- [21] A.R. Hipkiss, Carnosine and protein carbonyl groups: a possible relationship, *Biochemistry (Mosc.)* 65 (7) (2000) 771–778.
- [22] A. Bierhaus, M.A. Hofmann, R. Ziegler, P.P. Nawroth, AGEs and their reaction with AGE-receptors in vascular disease and diabetes mellitus. I. The AGE concept, *Cardiovasc. Res.* 37 (1998) 586–600.
- [23] L. Stryer, *Biochemistry*, third ed., Freeman, New York, 1988.
- [24] H.C. Gaede, W.-M. Yau, K. Gawrisch, Interaction between aromatic compounds and phospholipid bilayers, Poster PH 348, 44th ENC, Savannah, GA, 2003.
- [25] L.A. Sebring, R.J. Huxtable, Low affinity binding of taurine to phospholiposomes and cardiac sarcolemma, *Biochem. Biophys. Acta* 884 (1986) 559–566.
- [26] A.M. Rubtsov, Molecular mechanisms of regulation of the activity of sarcoplasmic Ca-release channels (ryanodine receptors), muscle fatigue, and Severin's phenomenon, *Biochemistry (Mosc.)* 66 (10) (2001) 1132–1143.
- [27] J.W. Pan, J.R. Hamm, D.L. Rothman, R.G. Shulman, Intracellular pH in human skeletal muscle by  $^1\text{H}$  NMR, *Proc. Natl. Acad. Sci. USA* 85 (1988) 7836–7839.
- [28] C.E. Brown, W.E. Antholine, Chelation chemistry of carnosine. Evidence that mixed complexes may occur in vivo, *J. Phys. Chem.* 83 (1979) 3314–3319.